

CANCOM2024 – CANADIAN INTERNATIONAL CONFERENCE ON COMPOSITE MATERIALS
**INVESTIGATION OF ANISOTROPIC THERMAL CONDUCTIVITY OF
3D-PRINTED CARBON FIBER REINFORCED POLYETHERIMIDE**

Ke, T¹, Azhdari, S¹, Margoto, OH², Szyplula, MM², Feuchtgruber, M³, Avalos, A⁴, Milani, AS², and Kravchenko, S¹

¹ Department of Materials Engineering, The University of British Columbia, Vancouver, Canada

² School of Engineering, The University of British Columbia, Okanagan, Canada

³ Chair of Carbon Composites, Technical University of Munich, Munich, Germany

⁴ AON3D, Montreal, Quebec, Canada

* Corresponding author (tt1224@student.ubc.ca)

Keywords: *Additive Manufacturing; Short Carbon Fiber Reinforced Polymer; Thermal Conductivity*

ABSTRACT

Understanding the thermal conductivity of 3D-printed carbon fiber (CF)/Polyetherimide (PEI) composites is important for maintaining the quality of the fabrication process. Additionally, in aerospace applications where CF/PEI is used for autoclave composite tooling, it is essential to understand how the thermal properties of the tooling material affect the heat distribution and curing process of the composite parts produced on these tools to optimize tooling design. This study investigates the anisotropic thermal conductivity of 3D-printed discontinuous CF/PEI composite, focusing on how the material microstructure affects thermal properties. A combination of experimental and numerical analysis was used. Thermal conductivity was measured using the Transient Plane Source (TPS) technique, and the microstructure was characterized to assess fiber length, orientation, volume fraction, and void content. The impact of these microstructural features on anisotropic thermal conductivity was then determined through numerical simulation using finite element analysis on the measured data. A successful tool has been established that implies the anisotropic thermal conductivity of short CF/PEI composites and how microstructure influences directional dependent thermal conductivities of short CF/PEI composites respectively. The results showed that an increase in CF volume fraction within the PEI/CF composites improved TC in the printing direction and increasing void content decreased the TC in all directions.

1 INTRODUCTION

In melt extrusion (ME) additive manufacturing (AM), also known as 3D printing, materials are introduced into a heated nozzle, melted, and selectively deposited in layers to construct a part, as shown schematically in Figure 1 (a). 3D printed fiber-reinforced polymer composites (FRPC) offer a lightweight yet robust solution for tooling for aerospace applications, enabling durable manufacturing processes. Thermal conductivity (TC) is significant in tooling as it influences efficient heat transfer, uniform heating/cooling and curing procedures, and even temperature distribution of the parts during the manufacturing process like autoclave manufacturing. Fused Filament Fabrication (FFF), or Filament-Based melt extrusion is a commonly used AM method that utilizes feedstock delivered to the nozzle in filament form [1]. Incorporating carbon fibers in the filament aims to enhance the thermal and mechanical properties of the parent polymer. Filaments for 3D printing are produced by extruding a mixture of thermoplastic and reinforcing materials, such as carbon fibers, through a die to form a continuous strand; during this process, voids typically develop due to uneven mixing, rapid cooling, or air entrapment [2]. During the printing process, the

CANCOM2024 – CANADIAN INTERNATIONAL CONFERENCE ON COMPOSITE MATERIALS

converging flow through the nozzle causes the fibers to align along the printing direction (x direction), creating preferential paths for heat transfer in that specific orientation, resulting in varying thermal conductivities along different axes. Figure 1(b) displays a micro-CT scan of a filament segment, wherein void (porosity) and short fiber content are evident. Therefore, post-printing, the microstructure of the composite showcases complexities such as random fiber orientation and void distribution, as illustrated by the micrographs in Figure 1(c). Due to the transverse isotropy of carbon fibers, the effective TC of the 3D-printed composites is orthotropic, which is determined by the fiber's volume fraction, orientation, and distribution of fibers and voids [3]. There has been previous work exploring how the thermal conductivity is affected by the matrix materials and geometry of the 3D-printed parts, however, less investigation on microstructure and morphology of 3D-printed short CFRPs on effective thermal conductivity has been carried out [4][5][6][7].

In this paper, a systematic study of the effective TC of a discontinuous short carbon fiber (CF) reinforced Polyetherimide (PEI) composite, manufactured with the FFF AM process, is presented. PEI, a high-temperature, amorphous thermoplastic commonly used in autoclave composite tooling manufacturing, offers the benefit of reduced shrinkage compared to semi-crystalline thermoplastics. The methodology combines (i) experimental measurement of TC in the x- (printing), y- (transverse), and z- (building) directions, as shown in Figure 1(a); (ii) detailed microstructural characterization; and (iii) finite element analysis to predict TC from measured microstructure parameters. Experimental work demonstrated that an 8% increase in CF volume fraction within the PEI/CF composites improved TC in the printing direction, while the results from numerical modeling highlighted that increasing the void content decreased the TC in all directions.

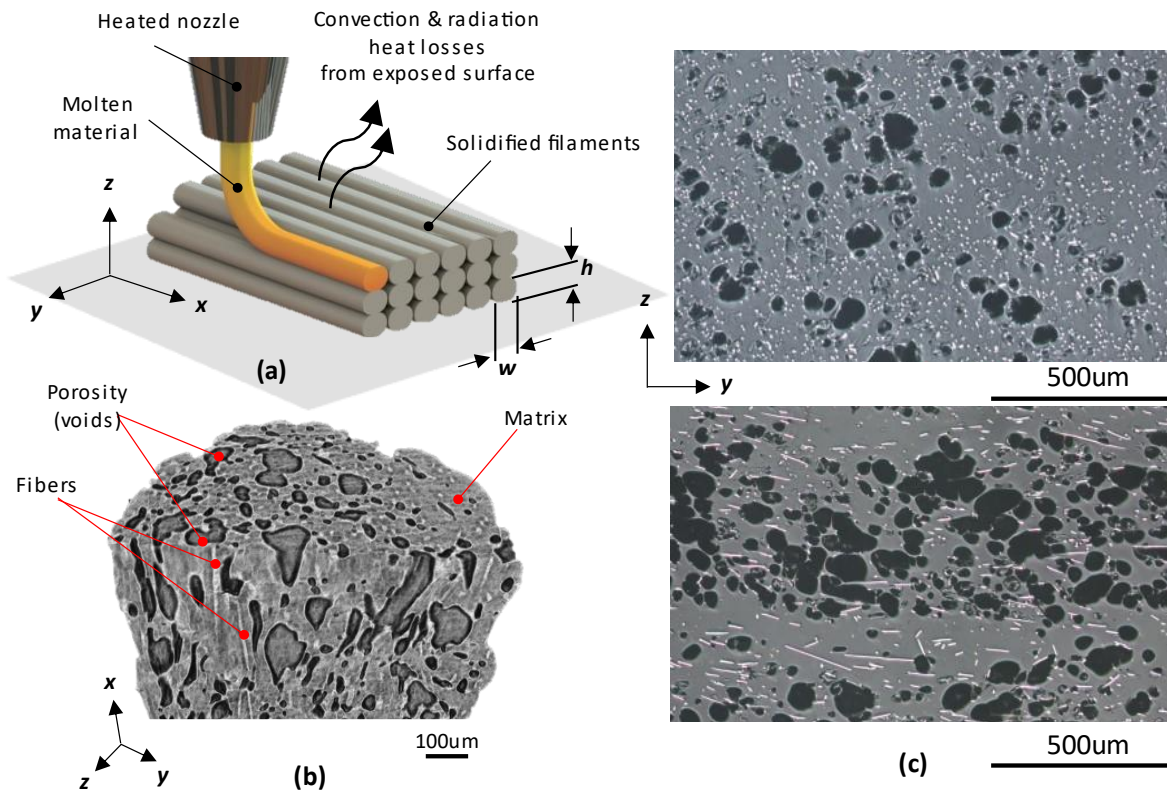


Figure 1. (a) ME AM process; (b) Micro-CT scan of a single filament segment; (c) Micrographs of the 3D-printed CFRP in printing direction x(up) and transverse direction y(down).

2 EXPERIMENTAL ANALYSIS

Samples used in the project were printed using an AON3D M2+ printer, utilizing ThermaX™ ULTEM 9085 PEI filament, and CarbonX™ ULTEM 9085 with 15% CF by mass. Before printing, the PEI filaments spool was dried at 90°C for 4 hours and stored in a dry box with molecular sieve desiccant to prevent moisture adsorption. The printer settings included a preheated bed temperature at 175°C and chamber temperature at 135°C for 2.5 hours, with extrusion temperature at 380°C for the first layer and 365°C thereafter; a nozzle size of 0.6mm; a bead width of 0.65 mm; a layer height of 0.3 mm; and print speed of 40mm/s in the aligned printing direction. The PEI and CF/PEI cubes were 2cm x 2cm x 2cm in dimension with the surfaces polished to ensure smooth surfaces for testing.

The experimental measurement of TC of the samples in this study was at 22°C by the Transient Plane Source (TPS) 2500S system which uses the transient-state heat transfer analysis from Hot Disk. By using a transient-state heat transfer method, a shorter time during the measurement was taken compared to other steady-state heat transfer methods [3]. This system employs a Kapton insulated sensor with a nickel heater in a dual spiral design of 3.189 mm radius (Hot Disk 5465) to measure the thermal conductivity of the 3D-printed composite samples. The sensor, functioning both as a heat source and a thermometer to measure the temperature of the samples, is sandwiched between two identical cubes, as shown in Figure 2(a). A clamping force of 25N is applied to the top specimen to ensure complete contact between the sensor and the specimens, as shown in Figure 2(b). During measurements, the sensor is powered and heated by an electric current, simultaneously recording the increase in temperature. As the sensor heats, its resistance and temperature change with time, providing the plot of temperature vs. time from which thermal conductivity is calculated. The heating power was set in the range of 20-25 mW. Measurement time was selected to 40s, to optimize the probe depth (heat dissipation depth) of the measurement. Since the heat propagates through the thickness, only the thermal conductivity in the heat dissipation direction can be measured and the measurement in other directions can be done by repositioning samples so that the direction of interest is perpendicular to the sensor. For thermal conductivity in each direction, 50 repeated measurements are done to decrease the instrumental errors. The TC of the neat PEI sample was measured at 0.214 W/mK. For the CF/PEI sample, TC was recorded at 0.304 W/mK, 0.234 W/mK, and 0.215 W/mK along the x-, y-, and z- directions, respectively, as presented in Figure 3(a).

The experimental characterization of the printed CF/PEI composite's microstructure included the analysis of fiber volume fraction (FVF), fiber orientation state, fiber diameter and length, and void volume content. Despite datasheets for commercially available filaments typically providing approximate fiber mass fractions, detailed microstructural information is missing. The sample size for the micro-CT scanning is around 4cm. The scans were performed by using a MicroXCT-400 system (supplier XRADIA) with a flat detector and no filter. The voltage, current, and power were set to 60 kV, 167 μA, and 10 W, respectively. Magnification of 20x was used, which resulted in a pixel size of 0.5μm, 2500 images were taken between 360 degrees and 130 source position projections were taken with an exposure time of 35 seconds. Commercially available software VG Studio Max was used to segment fibers in micro-CT images, further applying algorithms to determine the orientation of each fiber p_i relative to a predefined coordinate system, see Figure 4(a). This data was used to calculate the fiber orientation tensor A , to quantify the overall alignment of N fibers within the scanned volume by (1):

$$A = \frac{1}{N} \sum_{k=1}^N (p_i p_j)_k = \begin{bmatrix} 0.79 & -0.01 & 0.01 \\ -0.01 & 0.11 & 0 \\ 0.01 & 0 & 0.1 \end{bmatrix} \quad \text{where} \quad p_i = \begin{Bmatrix} p_1 \\ p_2 \\ p_3 \end{Bmatrix} = \begin{Bmatrix} \sin \theta \cos \varphi \\ \sin \theta \sin \varphi \\ \cos \theta \end{Bmatrix} \quad (1)$$

VG Studio analysis of micro-CT images quantified the porosity/void and fiber volume fractions at 25% and 8%, respectively. An average fiber diameter of 6 μm was assessed using micrographs. Fiber length was determined through a matrix carbonization test, which involved burning off the polymer matrix at 600°C for 1 hour to isolate the fibers;

CANCOM2024 – CANADIAN INTERNATIONAL CONFERENCE ON COMPOSITE MATERIALS

these residual fibers were then spread on a slide and measured to assess their average length of 67 μm under micrograph.

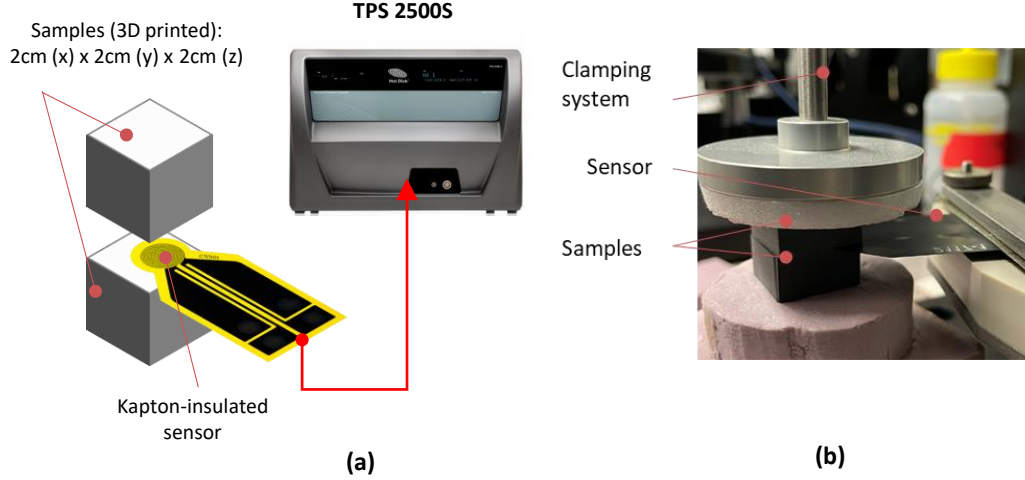


Figure 2. Schematic (a) and a photograph (b) of the TC measurement set-up (TPS2500 instrument).

3 NUMERICAL ANALYSIS

A finite element (FE) based model is developed to calculate the thermal conductivity of fiber-reinforced polymer composites using measured microstructure data. The model utilizes representative volume element (RVE) analysis that incorporates microstructural features to represent the physical composition of the material microscopically. The RVE geometry and finite element mesh were generated using DIGIMAT, which facilitated the input of fiber and void content, as measured in the previous section. An averaged diameter of the voids was 0.108 mm and randomly located in the RVE model. An example of the geometry and mesh is shown in Figure 4(b). The RVE dimensions are defined as $L_x \times L_y \times L_z = 100\mu\text{m} \times 100\mu\text{m} \times 50\mu\text{m}$ [8]. This mesh was exported to Abaqus/Standard (Implicit) to conduct a steady-state heat transfer analysis using DC3D4 elements, 4-node linear tetrahedral elements with temperature degrees of freedom. Material properties defined for the analysis including the density, specific heat, and thermal conductivity of PEI (matrix) are 1270 kg/m^3 , 2000 $\text{J}/(\text{kgK})$, 0.22 $\text{W}/(\text{mK})$ respectively (at room temperature); the density and specific heat of carbon fiber are 1790 kg/m^3 and 1134 $\text{J}/(\text{kgK})$, the transverse and axial thermal conductivity of carbon fiber are 2.108 $\text{W}/(\text{mK})$ and 6.83 $\text{W}/(\text{mK})$, respectively (at room temperature) [3]. For composite TC calculation in the x-direction, a steady-state heat transfer analysis was conducted. The boundary conditions implemented were: (i) isothermal conditions on the opposing surfaces in the x-direction, with temperature difference set as $T(x = 0) = T_0$ and $T(x = L_x) = T_1$, $\Delta T_x = T_1 - T_0$; (ii) adiabatic conditions on all other surfaces, ensuring no heat flux through these boundaries ($\partial T / \partial n = 0$, wherein n is the face normal). From the FE solution, the total average heat flux \bar{q}_x is calculated by solving the steady-state heat diffusion equation. The effective thermal conductivity in the x-direction, k_{xx} , was then calculated using Fourier's Law (2):

$$k_{xx} = -\frac{\bar{q}_x L_x}{\Delta T_x} \text{ where } \bar{q}_x = \frac{1}{A} \int q_x dA \quad (2)$$

CANCOM2024 – CANADIAN INTERNATIONAL CONFERENCE ON COMPOSITE MATERIALS

where A is the area of the surface that temperature is applied on; q_x is the local heat flux obtained from the FE solution; L_x is the length between the faces with the temperature difference. This procedure was repeated for the y - and z -directions to evaluate the k_{yy} and k_{zz} thermal properties of the composite.

Figure 3(a) compares experimental and numerical results for the thermal conductivity of PEI and its composites across three axes: x , y , and z . Both analyses demonstrate that thermal conductivity is highest in the x -direction, due to the alignment of carbon fibers, which have significantly higher thermal conductivity than the PEI matrix. The results across the y and z axes show minimal differences, indicating that fiber orientation primarily affects conductivity along the printing direction.

Using a computational model allows for the segregation of effects from different microstructural features of the composite, such as fibers and voids, on thermal conductivity. As reported in Figure 3(b), the addition of 8% carbon fibers, assuming no voids, significantly enhances thermal conductivity to $k_{xx} = 0.468 \text{ W/mK}$ in the x -, $k_{yy} = 0.264 \text{ W/mK}$ in y - and $k_{zz} = 0.256 \text{ W/mK}$ in the z -direction. This represents significantly higher conductivity in the x -direction compared to neat PEI ($k=0.214 \text{ W/mK}$) by a factor of close to 2 and notable improvements in the y and z directions. Conversely, when the polymer matrix includes 25% voids, the effective thermal conductivity is nearly isotropic and decreases to around 0.15 W/mK . This outcome illustrates that while carbon fibers can significantly increase thermal conductivity, particularly along the direction of fiber alignment, the presence of porosity substantially counteracts with these enhancements, resulting in a decreased overall effective thermal conductivity of the composite.

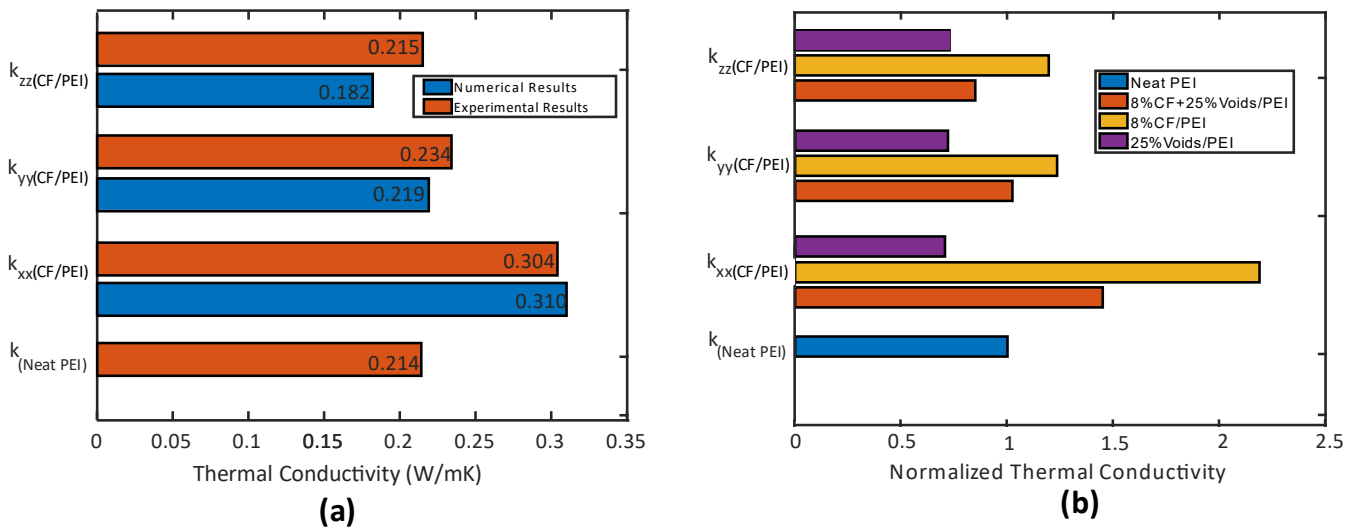


Figure 3. (a) Thermal conductivity of PEI and CF/PEI, experimental vs. simulation; (b) Simulated TC of CF/PEI composite as a function of various microstructural parameters.

4 CONCLUSION

This work gave an overview of how microstructure differs in the CFRP samples printed by filament-based melt extrusion method. A successful simulation model has been established that implies effective thermal conductivity in different directions of short CFRP composites and how microstructure influences thermal conductivities in 3 axial directions of 3D-printed short CFRP composites respectively. Both experimental and numerical results showed that an 8% increase in CF volume fraction along with 25% void volume content within the PEI/CF composites improved

CANCOM2024 – CANADIAN INTERNATIONAL CONFERENCE ON COMPOSITE MATERIALS

TC by a factor of 1.5 in the printing direction. Future works include the improvement of thermal conductivity by optimizing the microstructure of the 3D-printed CFRP composite and the possibility of making tools that have thermal conductivities differently from position to position in the required structure, which can be further researched.

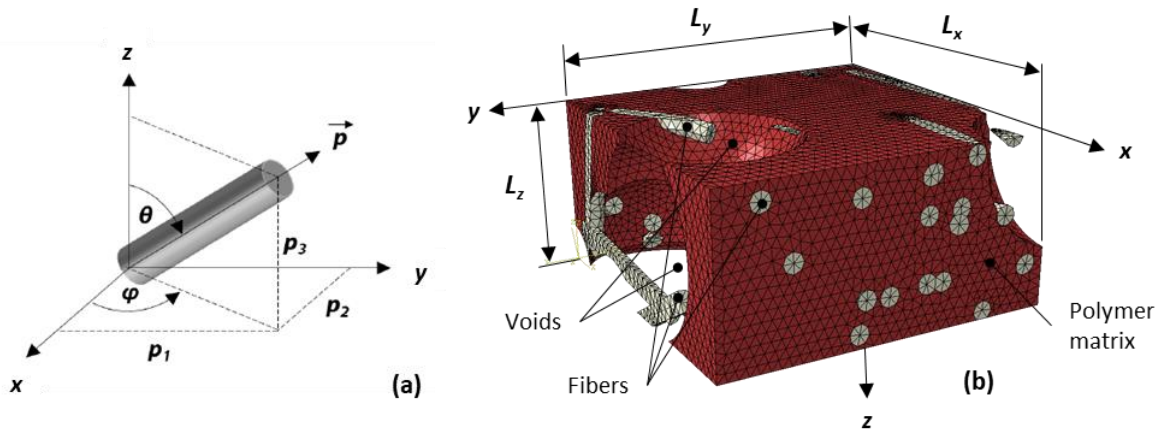


Figure 4. (a) Definition of Eulerian angle showing components of the fiber unit vector; (b) Experimental RVE of composite microstructure.

5 REFERENCES

- [1] Materials, A. S. for T. "Standard Terminology for Additive Manufacturing Technologies: ASTM F2792-12A". ASTM International, 2012.
- [2] R. Michaels, C. Wallace, A. R. Powell, K. Koka, K. Cohen, Z. Nourmohammadi, G.E. Green, and D. Zopf. "3D printing in surgical simulation: emphasized importance in the COVID-19 pandemic era". *Journal of 3D Printing in Medicine*, Vol. 5, No. 1, pp 5–9, 2021.
- [3] W. Chen, and D. Zhang. "A micromechanics-based processing model for predicting residual stress in fiber-reinforced polymer matrix composites". *Composite Structures*, Vol. 204, 153–166, 2018b.
- [4] L. Trhlíková, O. Zmeškal, P. Psencik, and P. Florián. "Study of the thermal properties of filaments for 3D printing". *AIP Conference Proceedings*. Terchova, Slovakia, Vol. 1752, 1, 2016.
- [5] C. Shemelya, Á. De La Rosa, A. R. Torrado, K. Yu, J. Domanowski, P.J. Bonacuse, R. E. Martin, M. Juhasz, F. I. Hurwitz, R.B. Wicker, B. Conner, E. MacDonald, and D. A. Roberson. "Anisotropy of thermal conductivity in 3D printed polymer matrix composites for space based cube satellites". *Additive Manufacturing*, Vol. 16, pp 186–196, 2017.
- [6] Y. Ibrahim, A. Elkholy, J. S. Schofield, G. W. Melenka, and R. Kemper. "Effective thermal conductivity of 3D-printed continuous fiber polymer composites". *Advanced Manufacturing*, Vol. 6, No. 1, pp 17–28, 2020.
- [7] I. Bute, S. Tarasovs, S. Vidinejevs, L. Vēvere, J. Sevchenko, and A. Aniskevich. "Thermal properties of 3D printed products from the most common polymers". *The International Journal of Advanced Manufacturing Technology*, Vol. 124, No. 7–8, pp 2739–2753, 2022.
- [8] D. Karimi, A. S. Milani. "SRVE modeling of particulate polymer matrix composites with irregularly shaped inclusions: Application to a green stone composite". *Composite Structures*, Vol. 228, No. 111331, 2019.